PHYSICAL REVIEW D **78,** 083529 (2008)

Planck priors for dark energy surveys

Pia Mukherjee,[1] Martin Kunz,[2] David Parkinson,[1] and Yun Wang[3]
[1]*Astronomy Centre, University of Sussex, Brighton BN1 9QH, United Kingdom*
[2]*Astronomy Centre, University of Sussex, Brighton BN1 9QH, United Kingdom; Department of Theoretical Physics, University of Geneva, 24 Quai E. Ansermet, 1211 Geneve 4, Switzerland*
[3]*Homer L. Dodge Department of Physics & Astronomy, University of Oklahoma, 440 W Brooks Street, Norman, Oklahoma, USA*
(Received 13 March 2008; published 20 October 2008)

Although cosmic microwave background anisotropy data alone cannot constrain simultaneously the spatial curvature and the equation of state of dark energy, CMB data provide a valuable addition to other experimental results. However computing a full CMB power spectrum with a Boltzmann code is quite slow; for instance if we want to work with many dark energy and/or modified gravity models, or would like to optimize experiments where many different configurations need to be tested, it is possible to adopt a quicker and more efficient approach. In this paper we consider the compression of the projected Planck cosmic microwave background data into four parameters, R (scaled distance to last scattering surface), l_a (angular scale of sound horizon at last scattering), $\Omega_b h^2$ (baryon density fraction) and n_s (powerlaw index of primordial matter power spectrum), all of which can be computed quickly. We show that, although this compression loses information compared to the full likelihood, such information loss becomes negligible when more data is added. We also demonstrate that the method can be used for canonical scalar-field dark energy independently of the parametrization of the equation of state, and discuss how this method should be used for other kinds of dark energy models.

DOI: 10.1103/PhysRevD.78.083529 PACS numbers: 98.80.Es, 95.36.+x, 98.70.Vc

I. INTRODUCTION

Dark energy model building continues to be an active area of research [1–10]. While current data remain consistent with a cosmological constant explanation for dark energy, other possibilities are not yet ruled out, especially if theoretical motivation can be found to tighten their predictions about the data [11]. New theoretical ideas thus may bolster support in favor of an exotic component of matter or a modification of gravity beyond some length scale.

On the observational front, recognizing the need for better data, many future dark energy surveys have been proposed, classified by the Dark Energy Task Force as stage III and stage IV experiments [12]. The realizable constraints from these surveys depend sensitively on the external or prior information that will be available in the future. A crucial external data set will come from the Planck satellite, which will place strong constraints on a range of cosmological parameters. It is therefore important to include this data for forecasts and optimizations of instrument performance for the stage III and IV dark energy surveys. This in turn requires a rapid way to evaluate the predicted Planck likelihood, preferably without the necessity to run a Boltzmann code.

Some of us have shown that the information from the WMAP CMB experiment [13] can be effectively and simply incorporated into a likelihood analysis of Type Ia supernovae (SN Ia) and baryon acoustic oscillation (BAO) data by including in the likelihood a term involving WMAP constraints on the CMB shift parameter (R), the angular scale of the sound horizon at last scattering (l_a), and the baryon density $\Omega_b h^2$, in Gaussian form together with their full covariance matrix [14]. The idea being that the calculation of full CMB spectra at each parameter point can be avoided, so that a Markov Chain Monte Carlo (MCMC) analysis proceeds very quickly. The merit lies in the method being independent of the dark energy model used as long as only background (or homogeneous) quantities are varied.

In this paper we extend the method to projected Planck data, which is significantly more accurate than WMAP data. We derive and test this simple prescription, compare it to a full likelihood analysis of simulated Planck data, and conclude that when such a Planck prior is combined with future dark energy surveys useful complementary information from the CMB is retained and there is no significant information loss. Hence the prescription remains an effective way to incorporate constraints from Planck (or Planck priors) in the analyses of data from future dark energy surveys.

II. COMPONENTS OF THE PROPOSED PLANCK LIKELIHOOD

Let us first introduce the parameters that we are proposing to use as an effective summary of the information contained in a CMB spectrum:

$$R \equiv \sqrt{\Omega_m H_0^2}\, r(z_{\rm CMB}), \qquad l_a \equiv \pi r(z_{\rm CMB})/r_s(z_{\rm CMB}), \quad (1)$$

where $r(z)$ is the comoving distance from the observer to redshift z, and $r_s(z_{\rm CMB})$ is the comoving size of the sound

horizon at decoupling. We give the details of the formulas used in Appendix A.

In this scheme, l_a describes the peak location through the angular diameter distance to decoupling and the size of the sound horizon at that time. If the geometry changes, either due to nonzero curvature or due to a different equation of state of dark energy, l_a changes in the same way as the peak structure. R encodes similar information, but in addition contains the matter density which is connected with the peak height. In a given class of models (for example, quintessence dark energy), these parameters are ''observables'' relating to the shape of the observed CMB spectrum, and constraints on them remain the same independent of (the prescription for) the equation of state of the dark energy. Furthermore, R and l_a are very well constrained by WMAP and even better by Planck and their likelihoods are almost perfectly Gaussian (remaining so under different treatments of dark energy), so that a Gaussian likelihood term together with the corresponding covariance matrix retains almost all of the information on these derived parameters. With curvature held fixed, an even simpler setup using just R sufficed and has been used by many authors, including [15,16].

As a caveat we note that if some assumptions regarding the evolution of perturbations are changed, then the corresponding R and l_a constraints and covariance matrix will need to be recalculated under each such hypothesis, for instance if massive neutrinos were to be included, or even if tensors were included in the analysis [17]. Further R as defined in Eq. (1) can be badly constrained and quite useless if the dark energy clusters as well, e.g. if it has a low sound speed, as in the model discussed in [18]. However, as discussed further below we checked that our constraints are valid at least for scalar-field dark energy models, independent of the parametrization of $w(z)$.

In addition to R and l_a we use the baryon density $\Omega_b h^2$, and optionally the spectral index of the scalar perturbations n_s, as these are strongly correlated with R and l_a, which means that we will lose information if we do not include these correlations.

III. SIMULATED DATA

Our simulation and treatment of Planck data is as in [19]. We include the temperature and polarization (TT, TE, and EE) spectra from three temperature channels with specification similar to the HFI channels of frequency 100 GHz, 143 GHz, and 217 GHz, and one 143 GHz polarization channel, following the current Planck documentation,[1] The full likelihood is constructed assuming a sky coverage of 0.8. We choose a fiducial model close to the WMAP best-fit LCDM model: $\Omega_b h^2 = 0.022$, $\Omega_m h^2 = 0.127$, $h = 0.73$, $\Omega_k = 0$, $w_0 = -1$, and $w_a = 0$.

[1] www.rssd.esa.int/index.php?project=PLANCK&page=perf_top

For the Baryon Acoustic Oscillation part, we use the experimental configuration outlined in the DETF report [12]. A Stage III spectroscopic experiment would cover 2000 square degrees with a redshift range of $0.5 < 1.3$, divided into 4 equally sized redshift bins, plus 300 square degrees with $2.3 < z < 3.3$. The experiment would obtain the spectra of 10^7 galaxies. This survey will measure the oscillations in the galaxy power spectrum, in the tangential direction (measuring $r(z)$), and the radial direction (measuring $dr(z)/dz = c/H(z)$, providing a direct measurement of the Hubble parameter). To estimate the accuracy with which the radial and tangential oscillations can be measured, we apply these survey parameters to the fitting formulas described in [20]. These fitting formulas only consider the accuracy with which the oscillations themselves can be measured, returning no information about the accuracy of the power spectrum measurement (as is done in e.g. [21,22]. This is because the number of possible parameters contributing to the nature of the matter power spectrum, such as running of the spectral index, massive neutrinos, and nonlinear bias, make this calculation very assumption dependent. In contrast, the positions of the oscillations are very robust with regard to these extra considerations.

For the supernovae, we use a Stage III spectroscopic survey as described in the DETF report [12]. We assume a scaled-up version of the SNLS survey with 2000 supernovae in the range $0.1 < z < 1$, with a further 500 supernovae at low redshift. The dispersion in observed magnitude is the sum in quadrature of a fixed $\sigma_D = 0.12$ with a second piece σ_m, which is fixed at 0.02 up to $z = 0.4$ but then increases up to 0.03 by $z = 1$.

IV. ANALYSIS

The full set of constraints on all parameters including R and l_a are determined through an MCMC-based likelihood analysis [23] of simulated Planck data. Planck will provide much tighter constraints on parameters, and its posterior will be significantly better localized in parameter space than that of WMAP. The shape of the posterior (i.e. parameter correlations) is also found to be quite different from WMAP's (further justifying the exercise of determining the best way to incorporate constraints from Planck separately from WMAP). While R and l_a were almost uncorrelated for WMAP data, this is no longer the case for Planck. Tables I and II show the estimated values and the covariance matrix for R, l_a, $\Omega_b h^2$ and n_s. In Table III we also show the normalized covariance matrix to illustrate the strong correlations between these parameters. We have included n_s here because it is found to have a correlation with R and l_a and a different consideration of BAO data in the future; utilizing the full shape of the matter power spectrum, might require the inclusion of n_s as a parameter. In the analysis presented in this paper, given the conserva-

TABLE I. R, l_a, $\Omega_b h^2$ and n_s estimated from Planck simulated data.

Parameter $\Omega_k \neq 0$	Mean	rms variance
R	1.7016	0.0055
l_a	302.108	0.098
$\Omega_b h^2$	0.02199	0.00017
n_s	0.9602	0.0038

tive treatment of the BAO signal, the inclusion of n_s does not have a noticeable impact.

The first point to consider and retest with Planck data is whether the constraints on R, l_a, $\Omega_b h^2$ and n_s, and their corresponding covariance matrix, are independent of the dark energy prescription used. In [14] we tested this for WMAP data for a cosmological constant, constant w and w_0-w_a models of dark energy, with and without curvature. Here we test it again for a flat model with a cosmological constant, and the w_0, w_a model and the kink model for dark energy, both with curvature, and for Planck quality data. In the w_0, w_a model $w_X(z) = w_0 + w_a(1-a)$ [24] which corresponds to $X(z) = a^{-3(1+w_0+w_a)} e^{3w_a(a-1)}$. In the kink model the equation of state parameter w_X is described by its value today, w_0, its asymptotic value at high redshift, w_m, as well by two more parameters giving the location and speed of the transition from w_m to w_0 [25]. In this case the energy density is derived through a numerical integration of the continuity equation. We found that there is no significant difference in the constraints on R, l_a, $\Omega_b h^2$ and n_s obtained using these different models. See Fig. 1.

Let us now test for the amount of information on parameters relevant to dark energy that is lost by considering a likelihood based on R, l_a, $\Omega_b h^2$ and n_s rather than the full CMB spectra. Figure 2 shows w_0, w_a contours obtained from a full likelihood analysis of Planck simulated data (shaded contours) against contours reconstructed from the R, l_a, $\Omega_b h^2$ and n_s likelihood (solid curves). We find that even in this limited 2D view there is significant information loss: The shaded contours from the full likelihood cover significantly less area than the open contours from the simpler likelihood. Because of the strong degeneracies which leave Planck basically unable to constrain cosmological parameters relating to dark energy and curvature on its own, the resulting contours depend strongly on the priors used.

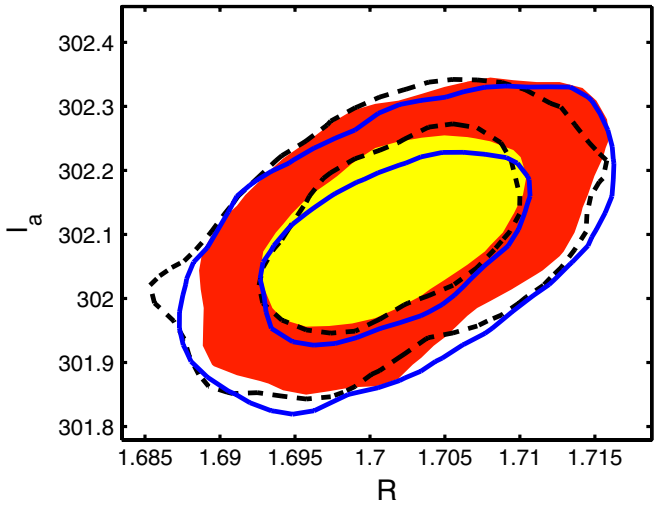

FIG. 1 (color online). This figure shows the projected 68% and 95% Planck constraints on R and l_a obtained assuming that dark energy was due to a cosmological constant (flat ΛCDM, dashed contours), a w_0, w_a model (shaded contours) and a kink model (solid contours), as described in the text.

Even though Planck on its own is not a very useful dark energy experiment, it will strongly improve the constraints from future dark energy probes like SN Ia and BAO. We show in Fig. 3 the marginalized 68% and 95% error contours for the combined BAO and SN Ia data sets, with and without adding the Planck data. We see that the constraints on w_0, w_a from a combined BAO and SN Ia data set are significantly improved when the Planck data is included. It is therefore important to include this additional information when optimizing or selecting future dark energy experiments.

It may be useful to note that given the R, l_a, $\Omega_b h^2$ and n_s likelihood, one can implement a full likelihood analysis under different dark energy models more efficiently using Hamiltonian Monte Carlo. In this method the R, l_a, $\Omega_b h^2$ and n_s likelihood is used as a guide to or an approximation of the true likelihood surface, but at each accepted point the likelihood is weighted using the full CMB spectra. We discuss this procedure in more detail in Appendix C.

However the question remains whether there is still an information loss when using the R, l_a, $\Omega_b h^2$ and n_s likelihood from Planck when analyzing SN Ia and/or BAO data, as compared to the full Boltzmann analysis of Planck data, which is much more time-consuming and so limits our ability to consider many varied dark energy models. To

TABLE II. Covariance matrix for $(R, l_a, \Omega_b h^2, n_s)$ from Planck.

$\Omega_k \neq 0$	R	l_a	$\Omega_b h^2$	n_s
R	0.303492E − 04	0.297688E − 03	−0.545532E − 06	−0.175976E − 04
l_a	0.297688E − 03	0.951881E − 02	−0.759752E − 05	−0.183814E − 03
$\Omega_b h^2$	−0.545532E − 06	−0.759752E − 05	0.279464E − 07	0.238882E − 06
n_s	−0.175976E − 04	−0.183814E − 03	0.238882E − 06	0.147219E − 04

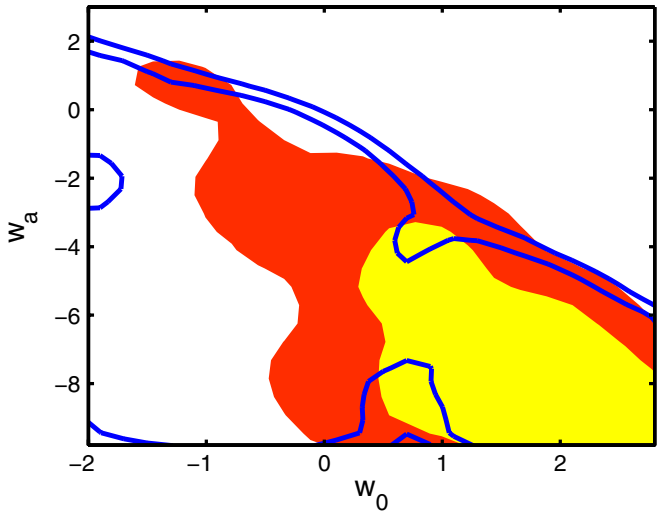

FIG. 2 (color online). This figure shows the Planck projected constraints on w_0, w_a obtained using a full likelihood analysis of simulated Planck data (shaded contours) and a simpler and quicker likelihood analysis based on R, l_a, $\Omega_b h^2$ and n_s (solid contours). Information is thus lost by the simplified analysis.

address this we compared the outputs from two analyses. First we performed a full MCMC run, i.e. including the full Planck likelihood and likelihoods from simulated stage III SN Ia and BAO surveys. Second we performed an MCMC analysis using the R, l_a, $\Omega_b h^2$ and n_s likelihood from Planck together with the SN Ia and BAO likelihood. Figure 4 shows the constraints obtained in each case. We conclude that there is effectively no information loss in using the R, l_a, $\Omega_b h^2$ and n_s likelihood, in conjunction with the likelihood from a better SN Ia and/or BAO ex-

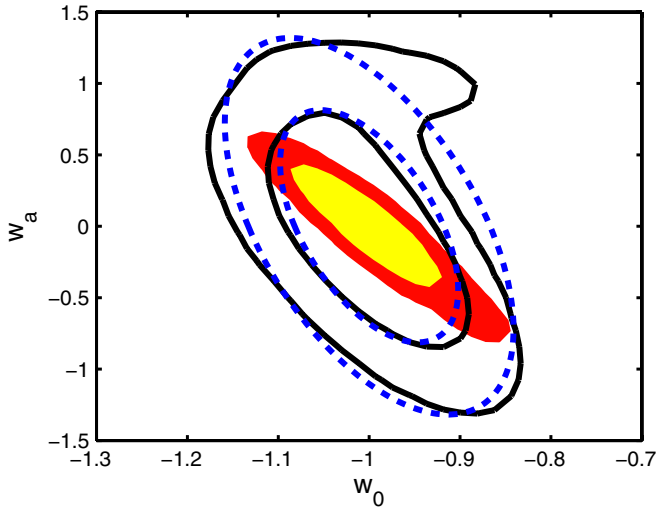

FIG. 3 (color online). This figure shows the projected constraints of stage III SN Ia and BAO experiments on w_0, w_a obtained using a full likelihood analysis (solid black contours) and a Fisher matrix analysis (dashed blue lines) and compares them to the constraints when this data is combined with the projected Planck data set (shaded contours).

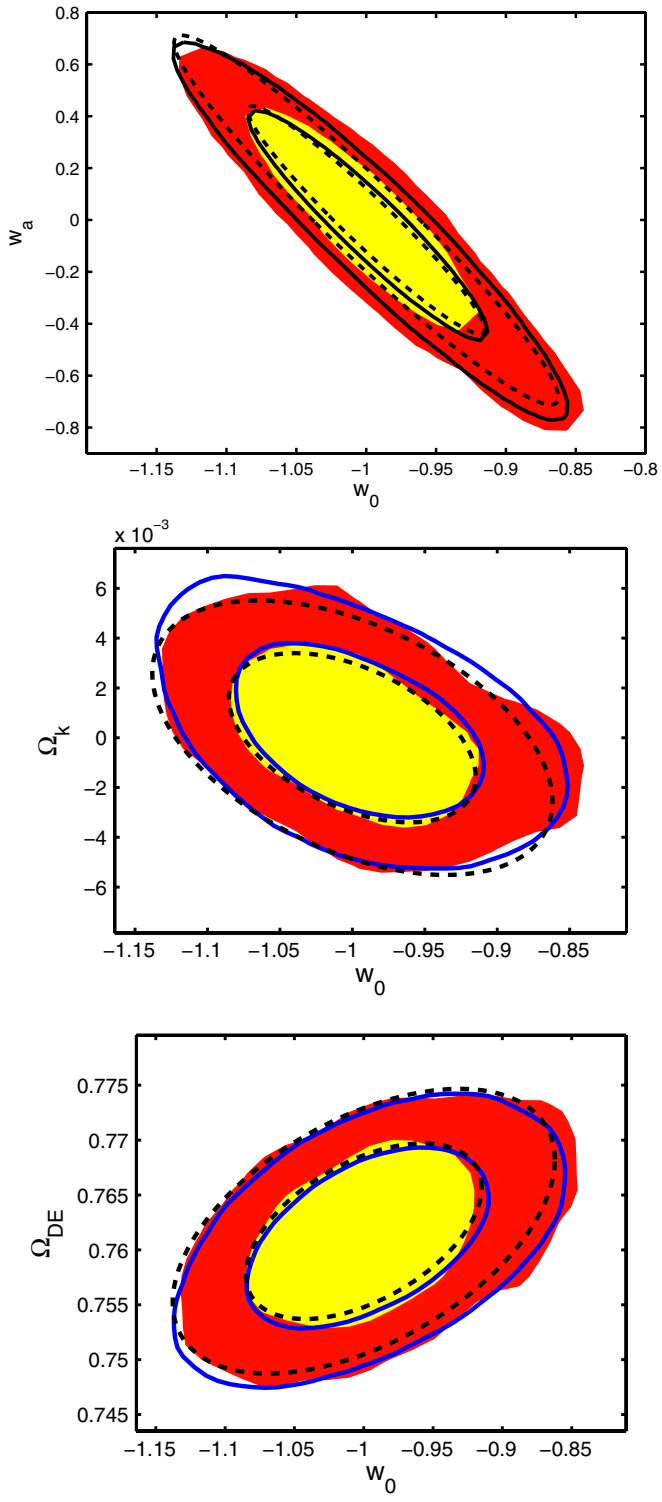

FIG. 4 (color online). This figure shows 2D confidence contours obtained using a full likelihood analysis of simulated Planck data in conjunction with stage III SN Ia and BAO data (shaded contours), contours obtained using the simplified R, l_a, $\Omega_b h^2$ and n_s based likelihood analysis of Planck data together with stage III SN Ia and BAO data (solid contours) and finally a Fisher matrix treatment of all data (dashed contours) as described further in the text.

TABLE III. Normalized covariance matrix for $(R, l_a, \Omega_b h^2, n_s)$ from Planck.

$\Omega_k \neq 0$	R	l_a	$\Omega_b h^2$	n_s
R	1.	0.553856	−0.592359	−0.832527
l_a	0.553856	1.	−0.465820	−0.491026
$\Omega_b h^2$	−0.592359	−0.465820	1.	0.372425
n_s	−0.832527	−0.491026	0.372425	1.

periment, and this condensed data analysis proceeds much faster than an analysis involving the full CMB likelihood.

Another way to include a Planck prior in forecasting constraints from a future dark energy experiment is to do it via a Planck Fisher matrix. Consider the above likelihood analysis in comparison to a Fisher matrix treatment. The Planck Fisher matrix was obtained from the Planck covariance matrix of $(R, l_a, \Omega_b h^2, n_s)$, with the appropriate parameter transformations for compatibility with the SN Ia and BAO Fisher matrices. See Appendix B for a description of how the Planck Fisher matrix was obtained and Table IV for the resulting Planck Fisher matrix. Constraints on dark energy parameters obtained in this way are also shown in Fig. 4. Because of the nearly unconstrained directions, the pure Planck Fisher matrix cannot be inverted, as the range of eigenvalues is larger than its precision. This can be rectified with weak priors on the parameters (in which case diagonal entries in the inverse of the Fisher matrix will reflect those priors), or by adding more data. Figure 3 shows that the Fisher matrix is valid in spite of its formal problems: the error contours for Planck + SN-Ia + BAO data agree very well with the others.

V. CONCLUSIONS

We have found that a Gaussian likelihood based on R, l_a, $\Omega_b h^2$ and n_s effectively summarizes the information in Planck that is relevant for an analysis of data from SN Ia and BAO experiments for dark energy parameters under different dark energy models. Therefore a Planck prior can be included in this manner. When used in conjunction with other data that are more sensitive to dark energy such a treatment of Planck data results in no information loss as compared to a full analysis, while being much faster.

We provide the full R, l_a, $\Omega_b h^2$, n_s covariance matrix that is required to define such a likelihood from Planck. We also provide a Planck Fisher matrix for people who prefer to use the Fisher matrix route to forecasting constraints for a future experiment. Using such a Planck prior we have obtained the type of constraints that may be expected from a stage III SN Ia and BAO survey. Of course the prescription can also be used once data from all these experiments have actually been obtained (i.e. the prescription is not just for forecasting).

In the above analysis we found that it was not strictly necessary to include n_s given our conservative treatment of BAO data. A fuller treatment of BAO data such as one that included the shape of the matter power spectrum rather than the transverse and line of sight distances to the redshifts of the BAO survey deduced from the BAO scales in the corresponding directions, would require the primordial power spectrum parameters including n_s to be considered a variable in the BAO part of the analysis. For this reason we have included n_s in our prescription, and marginalized over it in our results.

While this work was in progress [17] considered a likelihood analysis involving the locations of the peaks and troughs in the CMB spectrum observed by WMAP to constrain dark energy parameters in combination with recent BAO data. This offers another way to include information from the CMB in a likelihood analysis of BAO and SN Ia data. It involves fitting formulas for the locations of the extrema presented in [26]. Fitting formulas have been derived to account for certain prerecombination effects that via the early ISW effect can affect the position of the first peak relative to the higher peaks. In our formalism we would have to recompute the R, l_a, $\Omega_b h^2$ and n_s constraints for each new prerecombination scenario, such as involving a nonzero neutrino mass, involving tensors and/or the running of the scalar spectral index, or else include these parameters in the covariance matrix. On the other hand, our approach is arguably simpler to implement, and at least as accurate within its domain of applicability (since it additionally uses R as an effective measure of peak height). Also in their approach new fitting formulas would have to be derived to take into account new physics that had not already been considered.

TABLE IV. Fisher matrix for $(w_0, w_a, \Omega_{DE}, \Omega_k, \omega_m, \omega_b, n_s)$ derived from the covariance matrix for $(R, l_a, \Omega_b h^2, n_s)$ from Planck.

	w_0	w_a	Ω_{DE}	Ω_k	ω_m	ω_b	n_s
w_0	.172276E + 06	.490320E + 05	.674392E + 06	−.208974E + 07	.325219E + 07	−.790504E + 07	−.549427E + 05
w_a	.490320E + 05	.139551E + 05	.191940E + 06	−.594767E + 06	.925615E + 06	−.224987E + 07	−.156374E + 05
Ω_{DE}	.674392E + 06	.191940E + 06	.263997E + 07	−.818048E + 07	.127310E + 08	−.309450E + 08	−.215078E + 06
Ω_k	−.208974E + 07	−.594767E + 06	−.818048E + 07	.253489E + 08	−.394501E + 08	.958892E + 08	.666335E + 06
ω_m	.325219E + 07	.925615E + 06	.127310E + 08	−.394501E + 08	.633564E + 08	−.147973E + 09	−.501247E + 06
ω_b	−.790504E + 07	−.224987E + 07	−.309450E + 08	.958892E + 08	−.147973E + 09	.405079E + 09	.219009E + 07
n_s	−.549427E + 05	−.156374E + 05	−.215078E + 06	.666335E + 06	−.501247E + 06	.219009E + 07	.242767E + 06

ACKNOWLEDGMENTS

We thank Pier-Stefano Corasaniti and Julien Larena for interesting discussions. M. K. acknowledges partial funding by the Swiss NSF. P. M. acknowledges the Department of Physics and Astronomy, University of Sussex, for support.

APPENDIX A: DETAILED DESCRIPTION AND FORMULAS

The Planck satellite will deliver data of such a high quality that even small changes in parameters like the CMB temperature can have a significant impact. For this reason we summarize here the relevant formulas used in this paper. Generally they are those used by CAMB.

The comoving distance to a redshift z is given by

$$r(z) = cH_0^{-1}|\Omega_k|^{-1/2}\mathrm{sinn}[|\Omega_k|^{1/2}\Gamma(z)]$$
$$\Gamma(z) = \int_0^z \frac{dz'}{E(z')}, \qquad E(z) = H(z)/H_0 \tag{A1}$$

where $\Omega_k = -k/H_0^2$ with k denoting the curvature constant, and $\mathrm{sinn}(x) = \sin(x), x, \sinh(x)$ for $\Omega_k < 0$, $\Omega_k = 0$, and $\Omega_k > 0$ respectively, and

$$E(z) = [\Omega_m(1+z)^3 + \Omega_{\mathrm{rad}}(1+z)^4 \tag{A2}$$
$$+ \Omega_k(1+z)^2 + \Omega_X X(z)]^{1/2} \tag{A3}$$

with $\Omega_X = 1 - \Omega_m - \Omega_{\mathrm{rad}} - \Omega_k$, and the dark energy density function $X(z) \equiv \rho_X(z)/\rho_X(0)$.

We calculate the distance to decoupling, z_{CMB}, via the fitting formula in [27]. CAMB [28] uses the same fitting formula. We note that simply using a constant for z_{CMB} results in a shift in the inferred values of the CMB shift parameters at levels of precision corresponding to Planck.

The comoving sound horizon at recombination is given by

$$r_s(z_{\mathrm{CMB}}) = \int_0^{t_{\mathrm{CMB}}} \frac{c_s dt}{a} = cH_0^{-1}\int_{z_{\mathrm{CMB}}}^{\infty} dz \frac{c_s}{E(z)},$$
$$= cH_0^{-1}\int_0^{a_{\mathrm{CMB}}} \frac{da}{\sqrt{3(1+\bar{R}_b a)a^4 E^2(z)}}, \tag{A4}$$

where a is the cosmic scale factor, $a_{\mathrm{CMB}} = 1/(1+z_{\mathrm{CMB}})$, and $a^4E^2(z) = \Omega_{\mathrm{rad}} + \Omega_m a + \Omega_k a^2 + \Omega_X X(z)a^4$. The radiation density is computed using the Stefan-Boltzmann formula from the CMB temperature, assuming 3.04 families of massless neutrini. The sound speed is $c_s = 1/\sqrt{3(1+\bar{R}_b a)}$, with $\bar{R}_b a = 3\rho_b/(4\rho_\gamma)$, $\bar{R}_b = 31500\Omega_b h^2 (T_{\mathrm{CMB}}/2.7\ \mathrm{K})^{-4}$.[2]

APPENDIX B: FISHER MATRIX APPROACH

The Fisher matrix, $F_{\alpha\beta}$, for a set of parameters $\mathbf{p}$ can be derived from the Fisher matrix, F_{ij}, for a set of equivalent parameters $\mathbf{q}$ as follows [22]

$$F_{\alpha\beta} = \sum_{ij} \frac{\partial p_i}{\partial q_\alpha} F_{ij} \frac{\partial p_j}{\partial q_\beta}. \tag{B1}$$

The Fisher matrix of $\mathbf{q} = (R, l_a, \omega_b, n_s)$ is the inverse of the covariance matrix of $\mathbf{q}$ (given in Tables I and II). Note that the CMB shift parameters R and l_a encode all the information on dark energy parameters. For any given dark energy model parametrized by the parameter set $\mathbf{p}_X$, the relevant Fisher matrix for $\mathbf{p} = (\mathbf{p}_X, \Omega_{DE}, \Omega_k, \omega_m, \omega_b, n_s)$ can be found using Eq. (B1). For the case most discussed in the literature, $w_X(z) = w_0 + w_a(1-a)$, $\mathbf{p}_X = (w_0, w_a)$.

In order to find the Fisher matrix for $(w_0, w_a, \Omega_{DE}, \Omega_k, \omega_m, \omega_b, n_s)$, the following derivatives are needed:

$$\frac{\partial R}{\partial w_i} = \frac{\partial T(z_{\mathrm{CMB}})}{\partial w_i}\sqrt{\Omega_m}\mathrm{cosn}[|\Omega_k|^{1/2}\Gamma(z_{\mathrm{CMB}})] \qquad \frac{\partial \ln R}{\partial \Omega_{DE}} = -\frac{1}{2\Omega_m} + |\Omega_k|^{1/2}\frac{\mathrm{cosn}[|\Omega_k|^{1/2}\Gamma(z_{\mathrm{CMB}})]}{\mathrm{sinn}[|\Omega_k|^{1/2}\Gamma(z_{\mathrm{CMB}})]}\frac{\partial\Gamma(z_{\mathrm{CMB}})}{\partial\Omega_{DE}}$$
$$\frac{\partial \ln R}{\partial \Omega_k} = -\frac{1}{2\Omega_m} - \frac{1}{2\Omega_k} + |\Omega_k|^{1/2}\frac{\mathrm{cosn}[|\Omega_k|^{1/2}\Gamma(z_{\mathrm{CMB}})]}{\mathrm{sinn}[|\Omega_k|^{1/2}\Gamma(z_{\mathrm{CMB}})]}\left[\frac{\partial\Gamma(z_{\mathrm{CMB}})}{\partial\Omega_k} + \frac{\Gamma(z_{\mathrm{CMB}})}{2\Omega_k}\right] \qquad \frac{\partial R}{\partial \omega_m} = 0, \qquad \frac{\partial R}{\partial \omega_b} = 0,$$
$$\frac{\partial R}{\partial n_s} = 0 \qquad \frac{\partial \ln l_a}{\partial w_i} = |\Omega_k|^{1/2}\frac{\mathrm{cosn}[|\Omega_k|^{1/2}\Gamma(z_{\mathrm{CMB}})]}{\mathrm{sinn}[|\Omega_k|^{1/2}\Gamma(z_{\mathrm{CMB}})]} \qquad \frac{\partial\Gamma(z_{\mathrm{CMB}})}{\partial w_i} - \frac{\partial \ln[H_0 r_s(z_{\mathrm{CMB}})]}{\partial w_i}$$
$$\frac{\partial \ln l_a}{\partial \Omega_{DE}} = |\Omega_k|^{1/2}\frac{\mathrm{cosn}[|\Omega_k|^{1/2}\Gamma(z_{\mathrm{CMB}})]}{\mathrm{sinn}[|\Omega_k|^{1/2}\Gamma(z_{\mathrm{CMB}})]} \qquad \frac{\partial\Gamma(z_{\mathrm{CMB}})}{\partial\Omega_{DE}} - \frac{\partial \ln[H_0 r_s(z_{\mathrm{CMB}})]}{\partial\Omega_{DE}} \tag{B2}$$
$$\frac{\partial \ln l_a}{\partial \Omega_k} = -\frac{1}{2\Omega_k} + |\Omega_k|^{1/2}\frac{\mathrm{cosn}[|\Omega_k|^{1/2}\Gamma(z_{\mathrm{CMB}})]}{\mathrm{sinn}[|\Omega_k|^{1/2}\Gamma(z_{\mathrm{CMB}})]}\left[\frac{\partial\Gamma(z_{\mathrm{CMB}})}{\partial\Omega_k} + \frac{\Gamma(z_{\mathrm{CMB}})}{2\Omega_k}\right] - \frac{\partial \ln[H_0 r_s(z_{\mathrm{CMB}})]}{\partial\Omega_k}$$
$$\frac{\partial \ln l_a}{\partial w_m} = -\frac{\partial \ln[H_0 r_s(z_{\mathrm{CMB}})]}{\partial w_m}, \qquad \frac{\partial \ln l_a}{\partial w_b} = -\frac{\partial \ln[H_0 r_s(z_{\mathrm{CMB}})]}{\partial w_b}, \qquad \frac{\partial l_a}{\partial n_s} = 0 \qquad \frac{\partial \omega_b}{\partial \omega_b} = 1, \qquad \frac{\partial \omega_b}{\partial p_i} = 0$$
$$(p_i \neq \omega_b) \qquad \frac{\partial n_s}{\partial n_s} = 1, \qquad \frac{\partial n_s}{\partial p_i} = 0 \qquad (p_i \neq n_s),$$

[2]We used a $T_{\mathrm{CMB}} = 2.726$, and $\bar{R}_b = 30000\Omega_b h^2$ as defined in CAMB, noting that precision can be improved by updating these definitions.

where $w_i = (w_0, w_a)$, and $\mathrm{cosn}(x) = \cos(x)$, x, $\cosh(x)$ for $\Omega_k < 0$, $\Omega_k = 0$, and $\Omega_k > 0$, respectively.

Note that in the limit of $\Omega_k = 0$,

$$\frac{\partial \ln R}{\partial \Omega_k} = \frac{\partial \ln \Gamma(z_{\mathrm{CMB}})}{\partial \Omega_k} - \frac{1}{2\Omega_m} + \frac{[\Gamma(z_{\mathrm{CMB}})]^2}{6}$$
$$\frac{\partial \ln l_a}{\partial \Omega_k} = \frac{\partial \ln \Gamma(z_{\mathrm{CMB}})}{\partial \Omega_k} - \frac{\partial \ln[H_0 r_s(z_{\mathrm{CMB}})]}{\partial \Omega_k} + \frac{[\Gamma(z_{\mathrm{CMB}})]^2}{6}. \tag{B3}$$

For the fiducial model considered in this paper, the Planck Fisher matrix for $(w_0, w_a, \Omega_{DE}, \Omega_k, \omega_m, \omega_b, n_s)$ is derived from the Planck covariance matrix of (R, l_a, ω_b, n_s) given in Table IV.

APPENDIX C: USING OUR LIKELIHOOD FOR HAMILTONIAN MONTE CARLO

While most cosmological codes use the standard Metropolis MCMC algorithm, there are other MC approaches which may provide faster exploration especially in high dimensions. One example is Hamiltonian Monte Carlo (HMC) [29,30] where each parameter θ_i acquires a partner corresponding to a momentum variable π_i, and the log-likelihood is regarded as a potential. The momenta are drawn from a univariate normal probability distribution and the next step in the MCMC exploration is chosen based on a Hamiltonian motion in this system, with total energy $E = p^2/2 + \chi^2(\theta)/2$. At the end the momenta are marginalized over, which provides an ensemble of samples of the remaining parameters which is drawn from the posterior distribution. The main advantage of the HMC method is that the Hamiltonian motion naturally follows even complicated shapes of the posterior and in principle every proposal is accepted. The main drawback is that, in order to follow the trajectory, one needs to evaluate the gradient of the log-likelihood with respect to the parameters for dozens of steps, for every single proposal. Each proposal therefore requires hundred(s) of likelihood evaluations if the gradient cannot be computed analytically.

Since we have a reasonable approximation of the likelihood, we can instead use this approximation to compute the gradients. This means that the motion follows the (R, l_a, ω_b, n_s) likelihood and at the end the approximate and the true likelihood are compared. If the true likelihood is worse than the approximate one, then we can either assign the ratio as a weight to the new point (importance sampling) or test for rejection with the usual criterion (rejection sampling). If the true likelihood is better, then we have to assign the ratio as a weight >1. For this to work we must ensure that the approximate likelihood does not exclude parameter regions that the true likelihood would allow.

In our case we find that the procedure works quite well for the case where the Planck data is combined with the SN Ia and BAO data, since there the information loss is negligible.[3] Indeed, we find about 20% efficiency (i.e. roughly every 5th proposal is accepted, or correspondingly, the average weight of each point is 0.2), which is very good, especially since we can move a long distance and obtain completely uncorrelated samples. Using only the Planck data, we lose a lot of information, and less than 2% of the proposals are accepted. This is still not too bad, considering the complexity of the shape of the posterior, and that the resulting samples are completely decorrelated. Additionally, burn-in is very quick for HMC and there is no need for initial runs to determine the optimal proposal matrix.

[3]We add additionally τ and $\ln A_s$ to the set of our parameters, and augment the (R, l_a, ω_b, n_s) likelihood with their 2×2 covariance matrix.

[1] M. Kunz and D. Sapone, Phys. Rev. Lett. **98**, 121301 (2007).
[2] S. M. Carroll, A. de Felice, V. Duvvuri, D. A. Easson, M. Trodden, and M. S. Turner, Phys. Rev. D **71**, 063513 (2005).
[3] V. K. Onemli and R. P. Woodard, Phys. Rev. D **70**, 107301 (2004).
[4] V. F. Cardone, C. Tortora, A. Troisi, and S. Capozziello, Phys. Rev. D **73**, 043508 (2006).
[5] E. W. Kolb, S. Matarrese, and A. Riotto, New J. Phys. **8**, 322 (2006).
[6] R. R. Caldwell, W. Komp, L. Parker, and D. A. T. Vanzella, Phys. Rev. D **73**, 023513 (2006).
[7] E. O. Kahya and V. K. Onemli, Phys. Rev. D **76**, 043512 (2007).
[8] A. de Felice, P. Mukherjee, and P. Wang, Phys. Rev. D **77**, 024017 (2008).
[9] T. Koivisto, D. F. Mota, Phys. Rev. D **75**, 023518 (2007).
[10] Y. J. Ng, Phys. Lett. B **657**, 10 (2007).
[11] A. R. Liddle, P. Mukherjee, D. Parkinson, and Y. Wang, Phys. Rev. D **74** 123506 (2006).
[12] A. Albrecht, G. Bernstein, R. Cahn, W. L. Freedman, J. Hewitt, W. Hu, J. Huth, M. Kamionkowski, E. W. Kolb, L. Knox, J. C. Mather, S. Staggs, and N. B. Suntzeff, arXiv: astro-ph/0609591.
[13] D. N. Spergel *et al.*, Astrophys. J. Suppl. Ser. **170**, 377 (2007).
[14] Y. Wang and P. Mukherjee, Phys. Rev. D **76**, 103533 (2007).
[15] Y. Wang and P. Mukherjee, Astrophys. J. **650**, 1 (2006).

[16] Y. Wang and P. Mukherjee, Astrophys. J. **606**, 654 (2004).
[17] P. S. Corasaniti and A. Melchiorri, Phys. Rev. D **77**, 103507 (2008).
[18] M. Kunz, arXiv:astro-ph/0702615.
[19] C. Pahud, A. R. Liddle, P. Mukherjee, and D. Parkinson, Phys. Rev. D **73**, 123524 (2006).
[20] C. Blake, D. Parkinson, B. Bassett, K. Glazebrook, M. Kunz, and R. C. Nichol, Mon. Not. R. Astron. Soc. **365**, 255 (2006).
[21] H. J. Seo and D. J. Eisenstein, Astrophys. J. **598**, 720 (2003).
[22] Y. Wang, Astrophys. J. **647**, 1 (2006).
[23] A. Lewis and S. Bridle, Phys. Rev. D **66**, 103511 (2002).
[24] M. Chevallier and D. Polarski, Int. J. Mod. Phys. D **10**, 213 (2001).
[25] P. S. Corasaniti, M. Kunz, D. Parkinson, E. J. Copeland, and B. A. Bassett, Phys. Rev. D **70**, 083006 (2004).
[26] M. Doran and M. Lilley, Mon. Not. R. Astron. Soc. **330**, 965 (2002).
[27] W. Hu and N. Sugiyama, Astrophys. J. **471**, 542 (1996).
[28] A. Lewis, A. Challinor, and A. Lasenby, Astrophys. J. **538**, 473 (2000).
[29] D. J. C. MacKay, *Information Theory, Inference, and Learning Algorithms* (Cambridge University Press, Cambridge, England, 2003).
[30] A. Hajian, Phys. Rev. D **75**, 083525 (2007).